

Measurement of  $e^+e^- \rightarrow \omega\pi^0\pi^0$  cross section at center-of-mass energies  
from 2.00 to 3.08 GeV

M. Ablikim<sup>1</sup>, M. N. Achasov<sup>10,b</sup>, P. Adlarson<sup>68</sup>, M. Albrecht<sup>4</sup>, R. Aliberti<sup>28</sup>, A. Amoroso<sup>67A,67C</sup>, M. R. An<sup>32</sup>, Q. An<sup>64,50</sup>, X. H. Bai<sup>58</sup>, Y. Bai<sup>49</sup>, O. Bakina<sup>29</sup>, R. Baldini Ferrolli<sup>23A</sup>, I. Balossino<sup>24A</sup>, Y. Ban<sup>39,i</sup>, V. Batotzkaya<sup>1,37</sup>, D. Becker<sup>28</sup>, K. Begzsuren<sup>26</sup>, N. Berger<sup>28</sup>, M. Bertani<sup>23A</sup>, D. Bettoni<sup>24A</sup>, F. Bianchi<sup>67A,67C</sup>, J. Bloms<sup>61</sup>, A. Bortone<sup>67A,67C</sup>, I. Boyko<sup>29</sup>, R. A. Briere<sup>5</sup>, A. Brueggemann<sup>61</sup>, H. Cai<sup>69</sup>, X. Cai<sup>1,50</sup>, A. Calcaterra<sup>23A</sup>, G. F. Cao<sup>1,55</sup>, N. Cao<sup>1,55</sup>, S. A. Cetin<sup>54A</sup>, J. F. Chang<sup>1,50</sup>, W. L. Chang<sup>1,55</sup>, G. Chelkov<sup>29,a</sup>, C. Chen<sup>36</sup>, G. Chen<sup>1</sup>, H. S. Chen<sup>1,55</sup>, M. L. Chen<sup>1,50</sup>, S. J. Chen<sup>35</sup>, T. Chen<sup>1</sup>, X. R. Chen<sup>25</sup>, X. T. Chen<sup>1</sup>, Y. B. Chen<sup>1,50</sup>, Z. J. Chen<sup>20,j</sup>, W. S. Cheng<sup>67C</sup>, G. Cibinetto<sup>24A</sup>, F. Cossio<sup>67C</sup>, J. J. Cui<sup>42</sup>, H. L. Dai<sup>1,50</sup>, J. P. Dai<sup>71</sup>, A. Dbeyssi<sup>14</sup>, R. E. de Boer<sup>4</sup>, D. Dedovich<sup>29</sup>, Z. Y. Deng<sup>1</sup>, A. Denig<sup>28</sup>, I. Denysenko<sup>29</sup>, M. Destefanis<sup>67A,67C</sup>, F. De Mori<sup>67A,67C</sup>, Y. Ding<sup>33</sup>, J. Dong<sup>1,50</sup>, L. Y. Dong<sup>1,55</sup>, M. Y. Dong<sup>1,50,55</sup>, X. Dong<sup>69</sup>, S. X. Du<sup>73</sup>, P. Egorov<sup>29,a</sup>, Y. L. Fan<sup>69</sup>, J. Fang<sup>1,50</sup>, S. S. Fang<sup>1,55</sup>, Y. Fang<sup>1</sup>, R. Farinelli<sup>24A</sup>, L. Fava<sup>67B,67C</sup>, F. Feldbauer<sup>4</sup>, G. Felici<sup>23A</sup>, C. Q. Feng<sup>64,50</sup>, J. H. Feng<sup>51</sup>, K. Fischer<sup>62</sup>, M. Fritsch<sup>4</sup>, C. D. Fu<sup>1</sup>, H. Gao<sup>55,h</sup>, Y. N. Gao<sup>39,i</sup>, Yang Gao<sup>64,50</sup>, S. Garbolino<sup>67C</sup>, I. Garzia<sup>24A,24B</sup>, P. T. Ge<sup>69</sup>, C. Geng<sup>51</sup>, E. M. Gersabeck<sup>59</sup>, A. Gilman<sup>62</sup>, K. Goetzen<sup>11</sup>, L. Gong<sup>33</sup>, W. X. Gong<sup>1,50</sup>, W. Gradl<sup>28</sup>, M. Greco<sup>67A,67C</sup>, M. H. Gu<sup>1,50</sup>, C. Y. Guan<sup>1,55</sup>, A. Q. Guo<sup>25</sup>, L. B. Guo<sup>34</sup>, R. P. Guo<sup>41</sup>, Y. P. Guo<sup>9,g</sup>, A. Guskov<sup>29,a</sup>, T. T. Han<sup>42</sup>, W. Y. Han<sup>32</sup>, X. Q. Hao<sup>15</sup>, F. A. Harris<sup>57</sup>, K. K. He<sup>47</sup>, K. L. He<sup>1,55</sup>, F. H. Heinsius<sup>4</sup>, C. H. Heinz<sup>28</sup>, Y. K. Heng<sup>1,50,55</sup>, C. Herold<sup>52</sup>, M. Himmelreich<sup>11,e</sup>, T. Holtmann<sup>4</sup>, G. Y. Hou<sup>1,55</sup>, Y. R. Hou<sup>55</sup>, Z. L. Hou<sup>1</sup>, H. M. Hu<sup>1,55</sup>, J. F. Hu<sup>48,k</sup>, T. Hu<sup>1,50,55</sup>, Y. Hu<sup>1</sup>, G. S. Huang<sup>64,50</sup>, K. X. Huang<sup>51</sup>, L. Q. Huang<sup>65</sup>, X. T. Huang<sup>42</sup>, Y. P. Huang<sup>1</sup>, Z. Huang<sup>39,i</sup>, T. Hussain<sup>66</sup>, N. Hüsken<sup>22,28</sup>, W. Imoehl<sup>22</sup>, M. Irshad<sup>64,50</sup>, J. Jackson<sup>22</sup>, S. Jaeger<sup>4</sup>, S. Janchiv<sup>26</sup>, Q. Ji<sup>1</sup>, Q. P. Ji<sup>15</sup>, X. B. Ji<sup>1,55</sup>, X. L. Ji<sup>1,50</sup>, Y. Y. Ji<sup>42</sup>, Z. K. Jia<sup>64,50</sup>, H. B. Jiang<sup>42</sup>, S. S. Jiang<sup>32</sup>, X. S. Jiang<sup>1,50,55</sup>, Y. Jiang<sup>55</sup>, J. B. Jiao<sup>42</sup>, Z. Jiao<sup>18</sup>, S. Jin<sup>35</sup>, Y. Jin<sup>58</sup>, M. Q. Jing<sup>1,55</sup>, T. Johansson<sup>68</sup>, N. Kalantar-Nayestanaki<sup>56</sup>, X. S. Kang<sup>33</sup>, R. Kappert<sup>56</sup>, M. Kavatsyuk<sup>56</sup>, B. C. Ke<sup>73</sup>, I. K. Keshk<sup>4</sup>, A. Khoukaz<sup>61</sup>, P. Kiese<sup>28</sup>, R. Kiuchi<sup>1</sup>, R. Kliemt<sup>11</sup>, L. Koch<sup>30</sup>, O. B. Kolcu<sup>54A</sup>, B. Kopf<sup>4</sup>, M. Kuemmel<sup>4</sup>, M. Kuessner<sup>4</sup>, A. Kupsc<sup>37,68</sup>, W. Kühn<sup>30</sup>, J. J. Lane<sup>59</sup>, J. S. Lange<sup>30</sup>, P. Larin<sup>14</sup>, A. Lavania<sup>21</sup>, L. Lavezzi<sup>67A,67C</sup>, Z. H. Lei<sup>64,50</sup>, H. Leithoff<sup>28</sup>, M. Lellmann<sup>28</sup>, T. Lenz<sup>28</sup>, C. Li<sup>40</sup>, C. Li<sup>36</sup>, C. H. Li<sup>32</sup>, Cheng Li<sup>64,50</sup>, D. M. Li<sup>73</sup>, F. Li<sup>1,50</sup>, G. Li<sup>1</sup>, H. Li<sup>44</sup>, H. Li<sup>64,50</sup>, H. B. Li<sup>1,55</sup>, H. J. Li<sup>15</sup>, H. N. Li<sup>48,k</sup>, J. Q. Li<sup>4</sup>, J. S. Li<sup>51</sup>, J. W. Li<sup>42</sup>, Ke Li<sup>1</sup>, L. J. Li<sup>1</sup>, L. K. Li<sup>1</sup>, Lei Li<sup>3</sup>, M. H. Li<sup>36</sup>, P. R. Li<sup>31,l,m</sup>, S. X. Li<sup>9</sup>, S. Y. Li<sup>53</sup>, T. Li<sup>42</sup>, W. D. Li<sup>1,55</sup>, W. G. Li<sup>1</sup>, X. H. Li<sup>64,50</sup>, X. L. Li<sup>42</sup>, Xiaoyu Li<sup>1,55</sup>, Z. Y. Li<sup>51</sup>, H. Liang<sup>64,50</sup>, H. Liang<sup>27</sup>, H. Liang<sup>1,55</sup>, Y. F. Liang<sup>46</sup>, Y. T. Liang<sup>25</sup>, G. R. Liao<sup>12</sup>, L. Z. Liao<sup>42</sup>, J. Libby<sup>21</sup>, A. Limphirat<sup>52</sup>, C. X. Lin<sup>51</sup>, D. X. Lin<sup>25</sup>, T. Lin<sup>1</sup>, B. J. Liu<sup>1</sup>, C. X. Liu<sup>1</sup>, D. Liu<sup>14,64</sup>, F. H. Liu<sup>45</sup>, Fang Liu<sup>1</sup>, Feng Liu<sup>6</sup>, G. M. Liu<sup>48,k</sup>, H. M. Liu<sup>1,55</sup>, Huanhuan Liu<sup>1</sup>, Huihui Liu<sup>16</sup>, J. B. Liu<sup>64,50</sup>, J. L. Liu<sup>65</sup>, J. Y. Liu<sup>1,55</sup>, K. Liu<sup>1</sup>, K. Y. Liu<sup>33</sup>, Ke Liu<sup>17</sup>, L. Liu<sup>64,50</sup>, M. H. Liu<sup>9,g</sup>, P. L. Liu<sup>1</sup>, Q. Liu<sup>55</sup>, S. B. Liu<sup>64,50</sup>, T. Liu<sup>9,g</sup>, W. K. Liu<sup>36</sup>, W. M. Liu<sup>64,50</sup>, X. Liu<sup>31,l,m</sup>, Y. Liu<sup>31,l,m</sup>, Y. B. Liu<sup>36</sup>, Z. A. Liu<sup>1,50,55</sup>, Z. Q. Liu<sup>42</sup>, X. C. Lou<sup>1,50,55</sup>, F. X. Lu<sup>51</sup>, H. J. Lu<sup>18</sup>, J. G. Lu<sup>1,50</sup>, X. L. Lu<sup>1</sup>, Y. Lu<sup>1</sup>, Y. P. Lu<sup>1,50</sup>, Z. H. Lu<sup>1</sup>, C. L. Luo<sup>34</sup>, M. X. Luo<sup>72</sup>, T. Luo<sup>9,g</sup>, X. L. Luo<sup>1,50</sup>, X. R. Lyu<sup>55</sup>, Y. F. Lyu<sup>36</sup>, F. C. Ma<sup>33</sup>, H. L. Ma<sup>1</sup>, L. L. Ma<sup>42</sup>, M. M. Ma<sup>1,55</sup>, Q. M. Ma<sup>1</sup>, R. Q. Ma<sup>1,55</sup>, R. T. Ma<sup>55</sup>, X. Y. Ma<sup>1,50</sup>, Y. Ma<sup>39,i</sup>, F. E. Maas<sup>14</sup>, M. Maggiora<sup>67A,67C</sup>, S. Maldaner<sup>4</sup>, S. Malde<sup>62</sup>, Q. A. Malik<sup>66</sup>, A. Mangoni<sup>23B</sup>, Y. J. Mao<sup>39,i</sup>, Z. P. Mao<sup>1</sup>, S. Marcello<sup>67A,67C</sup>, Z. X. Meng<sup>58</sup>, J. G. Messchendorp<sup>56,d</sup>, G. Mezzadri<sup>24A</sup>, H. Miao<sup>1</sup>, T. J. Min<sup>35</sup>, R. E. Mitchell<sup>22</sup>, X. H. Mo<sup>1,50,55</sup>, N. Yu. Muchnoi<sup>10,b</sup>, H. Muramatsu<sup>60</sup>, Y. Nefedov<sup>29</sup>, F. Nerling<sup>11,e</sup>, I. B. Nikolaev<sup>10,b</sup>, Z. Ning<sup>1,50</sup>, S. Nisar<sup>8,n</sup>, Y. Niu<sup>42</sup>, S. L. Olsen<sup>55</sup>, Q. Ouyang<sup>1,50,55</sup>, S. Pacetti<sup>23B,23C</sup>, X. Pan<sup>9,g</sup>, Y. Pan<sup>59</sup>, A. Pathak<sup>1</sup>, A. Pathak<sup>27</sup>, M. Pelizaeus<sup>4</sup>, H. P. Peng<sup>64,50</sup>, K. Peters<sup>11,e</sup>, J. Pettersson<sup>68</sup>, J. L. Ping<sup>34</sup>, R. G. Ping<sup>1,55</sup>, S. Plura<sup>28</sup>, S. Pogodin<sup>29</sup>, R. Poling<sup>60</sup>, V. Prasad<sup>64,50</sup>, H. Qi<sup>64,50</sup>, H. R. Qi<sup>53</sup>, M. Qi<sup>35</sup>, T. Y. Qi<sup>9,g</sup>, S. Qian<sup>1,50</sup>, W. B. Qian<sup>55</sup>, Z. Qian<sup>51</sup>, C. F. Qiao<sup>55</sup>, J. J. Qin<sup>65</sup>, L. Q. Qin<sup>12</sup>, X. P. Qin<sup>9,g</sup>, X. S. Qin<sup>42</sup>, Z. H. Qin<sup>1,50</sup>, J. F. Qiu<sup>1</sup>, S. Q. Qu<sup>36</sup>, S. Q. Qu<sup>53</sup>, K. H. Rashid<sup>66</sup>, K. Ravindran<sup>21</sup>, C. F. Redmer<sup>28</sup>, K. J. Ren<sup>32</sup>, A. Rivetti<sup>67C</sup>, V. Rodin<sup>56</sup>, M. Rolo<sup>67C</sup>, G. Rong<sup>1,55</sup>, Ch. Rosner<sup>14</sup>, H. S. Sang<sup>64</sup>, A. Sarantsev<sup>29,c</sup>, Y. Schelhaas<sup>28</sup>, C. Schnier<sup>4</sup>, K. Schoenning<sup>68</sup>, M. Scodreggio<sup>24A,24B</sup>, K. Y. Shan<sup>9,g</sup>, W. Shan<sup>19</sup>, X. Y. Shan<sup>64,50</sup>, J. F. Shangguan<sup>47</sup>, L. G. Shao<sup>1,55</sup>, M. Shao<sup>64,50</sup>, C. P. Shen<sup>9,g</sup>, H. F. Shen<sup>1,55</sup>, X. Y. Shen<sup>1,55</sup>, B.-A. Shi<sup>55</sup>, H. C. Shi<sup>64,50</sup>, R. S. Shi<sup>1,55</sup>, X. Shi<sup>1,50</sup>, X. D. Shi<sup>64,50</sup>, J. J. Song<sup>15</sup>, W. M. Song<sup>27,1</sup>, Y. X. Song<sup>39,i</sup>, S. Sosio<sup>67A,67C</sup>, S. Spataro<sup>67A,67C</sup>, F. Stieler<sup>28</sup>, K. X. Su<sup>69</sup>, P. P. Su<sup>47</sup>, Y.-J. Su<sup>55</sup>, G. X. Sun<sup>1</sup>, H. Sun<sup>55</sup>, H. K. Sun<sup>1</sup>, J. F. Sun<sup>15</sup>, L. Sun<sup>69</sup>, S. S. Sun<sup>1,55</sup>, T. Sun<sup>1,55</sup>, W. Y. Sun<sup>27</sup>, X. Sun<sup>20,j</sup>, Y. J. Sun<sup>64,50</sup>, Y. Z. Sun<sup>1</sup>, Z. T. Sun<sup>42</sup>, Y. H. Tan<sup>69</sup>, Y. X. Tan<sup>64,50</sup>, C. J. Tang<sup>46</sup>, G. Y. Tang<sup>1</sup>, J. Tang<sup>51</sup>, L. Y. Tao<sup>65</sup>, Q. T. Tao<sup>20,j</sup>, J. X. Teng<sup>64,50</sup>, V. Thoren<sup>68</sup>, W. H. Tian<sup>44</sup>, Y. T. Tian<sup>25</sup>, I. Uman<sup>54B</sup>, B. Wang<sup>1</sup>, D. Y. Wang<sup>39,i</sup>, F. Wang<sup>65</sup>, H. J. Wang<sup>31,l,m</sup>, H. P. Wang<sup>1,55</sup>, K. Wang<sup>1,50</sup>, L. L. Wang<sup>1</sup>, M. Wang<sup>42</sup>, M. Z. Wang<sup>39,i</sup>, Meng Wang<sup>1,55</sup>, S. Wang<sup>9,g</sup>, T. J. Wang<sup>36</sup>, W. Wang<sup>51</sup>, W. H. Wang<sup>69</sup>, W. P. Wang<sup>64,50</sup>,

X. Wang<sup>39,i</sup>, X. F. Wang<sup>31,l,m</sup>, X. L. Wang<sup>9,g</sup>, Y. D. Wang<sup>38</sup>, Y. F. Wang<sup>1,50,55</sup>, Y. H. Wang<sup>40</sup>, Y. Q. Wang<sup>1</sup>, Y. Y. Wang<sup>31,l,m</sup>, Ying Wang<sup>51</sup>, Z. Wang<sup>1,50</sup>, Z. Y. Wang<sup>1</sup>, Ziyi Wang<sup>55</sup>, D. H. Wei<sup>12</sup>, F. Weidner<sup>61</sup>, S. P. Wen<sup>1</sup>, D. J. White<sup>59</sup>, U. Wiedner<sup>4</sup>, G. Wilkinson<sup>62</sup>, M. Wolke<sup>68</sup>, L. Wollenberg<sup>4</sup>, J. F. Wu<sup>1,55</sup>, L. H. Wu<sup>1</sup>, L. J. Wu<sup>1,55</sup>, X. Wu<sup>9,g</sup>, X. H. Wu<sup>27</sup>, Y. Wu<sup>64</sup>, Z. Wu<sup>1,50</sup>, L. Xia<sup>64,50</sup>, T. Xiang<sup>39,i</sup>, H. Xiao<sup>9,g</sup>, S. Y. Xiao<sup>1</sup>, Y. L. Xiao<sup>9,g</sup>, Z. J. Xiao<sup>34</sup>, X. H. Xie<sup>39,i</sup>, Y. Xie<sup>42</sup>, Y. G. Xie<sup>1,50</sup>, Y. H. Xie<sup>6</sup>, Z. P. Xie<sup>64,50</sup>, T. Y. Xing<sup>1,55</sup>, C. F. Xu<sup>1</sup>, C. J. Xu<sup>51</sup>, G. F. Xu<sup>1</sup>, Q. J. Xu<sup>13</sup>, S. Y. Xu<sup>63</sup>, X. P. Xu<sup>47</sup>, Y. C. Xu<sup>55</sup>, F. Yan<sup>9,g</sup>, L. Yan<sup>9,g</sup>, W. B. Yan<sup>64,50</sup>, W. C. Yan<sup>73</sup>, H. J. Yang<sup>43,f</sup>, H. L. Yang<sup>27</sup>, H. X. Yang<sup>1</sup>, L. Yang<sup>44</sup>, S. L. Yang<sup>55</sup>, Y. X. Yang<sup>1,55</sup>, Yifan Yang<sup>1,55</sup>, M. Ye<sup>1,50</sup>, M. H. Ye<sup>7</sup>, J. H. Yin<sup>1</sup>, Z. Y. You<sup>51</sup>, B. X. Yu<sup>1,50,55</sup>, C. X. Yu<sup>36</sup>, G. Yu<sup>1,55</sup>, J. S. Yu<sup>20,j</sup>, T. Yu<sup>65</sup>, C. Z. Yuan<sup>1,55</sup>, L. Yuan<sup>2</sup>, S. C. Yuan<sup>1</sup>, X. Q. Yuan<sup>1</sup>, Y. Yuan<sup>1,55</sup>, Z. Y. Yuan<sup>51</sup>, C. X. Yue<sup>32</sup>, A. A. Zafar<sup>66</sup>, F. R. Zeng<sup>42</sup>, X. Zeng Zeng<sup>6</sup>, Y. Zeng<sup>20,j</sup>, Y. H. Zhan<sup>51</sup>, A. Q. Zhang<sup>1</sup>, B. L. Zhang<sup>1</sup>, B. X. Zhang<sup>1</sup>, G. Y. Zhang<sup>15</sup>, H. Zhang<sup>64</sup>, H. H. Zhang<sup>27</sup>, H. H. Zhang<sup>51</sup>, H. Y. Zhang<sup>1,50</sup>, J. L. Zhang<sup>70</sup>, J. Q. Zhang<sup>34</sup>, J. W. Zhang<sup>1,50,55</sup>, J. Y. Zhang<sup>1</sup>, J. Z. Zhang<sup>1,55</sup>, Jianyu Zhang<sup>1,55</sup>, Jiawei Zhang<sup>1,55</sup>, L. M. Zhang<sup>53</sup>, L. Q. Zhang<sup>51</sup>, Lei Zhang<sup>35</sup>, P. Zhang<sup>1</sup>, Shulei Zhang<sup>20,j</sup>, X. D. Zhang<sup>38</sup>, X. M. Zhang<sup>1</sup>, X. Y. Zhang<sup>47</sup>, X. Y. Zhang<sup>42</sup>, Y. Zhang<sup>62</sup>, Y. T. Zhang<sup>73</sup>, Y. H. Zhang<sup>1,50</sup>, Yan Zhang<sup>64,50</sup>, Yao Zhang<sup>1</sup>, Z. H. Zhang<sup>1</sup>, Z. Y. Zhang<sup>69</sup>, Z. Y. Zhang<sup>36</sup>, G. Zhao<sup>1</sup>, J. Zhao<sup>32</sup>, J. Y. Zhao<sup>1,55</sup>, J. Z. Zhao<sup>1,50</sup>, Lei Zhao<sup>64,50</sup>, Ling Zhao<sup>1</sup>, M. G. Zhao<sup>36</sup>, Q. Zhao<sup>1</sup>, S. J. Zhao<sup>73</sup>, Y. B. Zhao<sup>1,50</sup>, Y. X. Zhao<sup>25</sup>, Z. G. Zhao<sup>64,50</sup>, A. Zhemchugov<sup>29,a</sup>, B. Zheng<sup>65</sup>, J. P. Zheng<sup>1,50</sup>, Y. H. Zheng<sup>55</sup>, B. Zhong<sup>34</sup>, C. Zhong<sup>65</sup>, X. Zhong<sup>51</sup>, H. Zhou<sup>42</sup>, L. P. Zhou<sup>1,55</sup>, X. Zhou<sup>69</sup>, X. K. Zhou<sup>55</sup>, X. R. Zhou<sup>64,50</sup>, X. Y. Zhou<sup>32</sup>, Y. Z. Zhou<sup>9,g</sup>, J. Zhu<sup>36</sup>, K. Zhu<sup>1</sup>, K. J. Zhu<sup>1,50,55</sup>, L. X. Zhu<sup>55</sup>, S. H. Zhu<sup>63</sup>, T. J. Zhu<sup>70</sup>, W. J. Zhu<sup>36</sup>, W. J. Zhu<sup>9,g</sup>, Y. C. Zhu<sup>64,50</sup>, Z. A. Zhu<sup>1,55</sup>, B. S. Zou<sup>1</sup>, J. H. Zou<sup>1</sup>

(BESIII Collaboration)

<sup>1</sup> *Institute of High Energy Physics, Beijing 100049, People's Republic of China*

<sup>2</sup> *Beihang University, Beijing 100191, People's Republic of China*

<sup>3</sup> *Beijing Institute of Petrochemical Technology, Beijing 102617, People's Republic of China*

<sup>4</sup> *Bochum Ruhr-University, D-44780 Bochum, Germany*

<sup>5</sup> *Carnegie Mellon University, Pittsburgh, Pennsylvania 15213, USA*

<sup>6</sup> *Central China Normal University, Wuhan 430079, People's Republic of China*

<sup>7</sup> *China Center of Advanced Science and Technology, Beijing 100190, People's Republic of China*

<sup>8</sup> *COMSATS University Islamabad, Lahore Campus, Defence Road, Off Raiwind Road, 54000 Lahore, Pakistan*

<sup>9</sup> *Fudan University, Shanghai 200433, People's Republic of China*

<sup>10</sup> *G.I. Budker Institute of Nuclear Physics SB RAS (BINP), Novosibirsk 630090, Russia*

<sup>11</sup> *GSI Helmholtzcentre for Heavy Ion Research GmbH, D-64291 Darmstadt, Germany*

<sup>12</sup> *Guangxi Normal University, Guilin 541004, People's Republic of China*

<sup>13</sup> *Hangzhou Normal University, Hangzhou 310036, People's Republic of China*

<sup>14</sup> *Helmholtz Institute Mainz, Staudinger Weg 18, D-55099 Mainz, Germany*

<sup>15</sup> *Henan Normal University, Xinxiang 453007, People's Republic of China*

<sup>16</sup> *Henan University of Science and Technology, Luoyang 471003, People's Republic of China*

<sup>17</sup> *Henan University of Technology, Zhengzhou 450001, People's Republic of China*

<sup>18</sup> *Huangshan College, Huangshan 245000, People's Republic of China*

<sup>19</sup> *Hunan Normal University, Changsha 410081, People's Republic of China*

<sup>20</sup> *Hunan University, Changsha 410082, People's Republic of China*

<sup>21</sup> *Indian Institute of Technology Madras, Chennai 600036, India*

<sup>22</sup> *Indiana University, Bloomington, Indiana 47405, USA*

<sup>23</sup> *INFN Laboratori Nazionali di Frascati, (A)INFN Laboratori Nazionali di Frascati, I-00044, Frascati, Italy;*

*(B)INFN Sezione di Perugia, I-06100, Perugia, Italy; (C)University of Perugia, I-06100, Perugia, Italy*

<sup>24</sup> *INFN Sezione di Ferrara, (A)INFN Sezione di Ferrara, I-44122,*

*Ferrara, Italy; (B)University of Ferrara, I-44122, Ferrara, Italy*

<sup>25</sup> *Institute of Modern Physics, Lanzhou 730000, People's Republic of China*

<sup>26</sup> *Institute of Physics and Technology, Peace Ave. 54B, Ulaanbaatar 13330, Mongolia*

<sup>27</sup> *Jilin University, Changchun 130012, People's Republic of China*

<sup>28</sup> *Johannes Gutenberg University of Mainz, Johann-Joachim-Becher-Weg 45, D-55099 Mainz, Germany*

<sup>29</sup> *Joint Institute for Nuclear Research, 141980 Dubna, Moscow region, Russia*

<sup>30</sup> *Justus-Liebig-Universitaet Giessen, II. Physikalisches Institut, Heinrich-Buff-Ring 16, D-35392 Giessen, Germany*

<sup>31</sup> *Lanzhou University, Lanzhou 730000, People's Republic of China*

- <sup>32</sup> Liaoning Normal University, Dalian 116029, People's Republic of China
- <sup>33</sup> Liaoning University, Shenyang 110036, People's Republic of China
- <sup>34</sup> Nanjing Normal University, Nanjing 210023, People's Republic of China
- <sup>35</sup> Nanjing University, Nanjing 210093, People's Republic of China
- <sup>36</sup> Nankai University, Tianjin 300071, People's Republic of China
- <sup>37</sup> National Centre for Nuclear Research, Warsaw 02-093, Poland
- <sup>38</sup> North China Electric Power University, Beijing 102206, People's Republic of China
- <sup>39</sup> Peking University, Beijing 100871, People's Republic of China
- <sup>40</sup> Qufu Normal University, Qufu 273165, People's Republic of China
- <sup>41</sup> Shandong Normal University, Jinan 250014, People's Republic of China
- <sup>42</sup> Shandong University, Jinan 250100, People's Republic of China
- <sup>43</sup> Shanghai Jiao Tong University, Shanghai 200240, People's Republic of China
- <sup>44</sup> Shanxi Normal University, Linfen 041004, People's Republic of China
- <sup>45</sup> Shanxi University, Taiyuan 030006, People's Republic of China
- <sup>46</sup> Sichuan University, Chengdu 610064, People's Republic of China
- <sup>47</sup> Soochow University, Suzhou 215006, People's Republic of China
- <sup>48</sup> South China Normal University, Guangzhou 510006, People's Republic of China
- <sup>49</sup> Southeast University, Nanjing 211100, People's Republic of China
- <sup>50</sup> State Key Laboratory of Particle Detection and Electronics, Beijing 100049, Hefei 230026, People's Republic of China
- <sup>51</sup> Sun Yat-Sen University, Guangzhou 510275, People's Republic of China
- <sup>52</sup> Suranaree University of Technology, University Avenue 111, Nakhon Ratchasima 30000, Thailand
- <sup>53</sup> Tsinghua University, Beijing 100084, People's Republic of China
- <sup>54</sup> Turkish Accelerator Center Particle Factory Group, (A)Istinye University, 34010, Istanbul, Turkey; (B)Near East University, Nicosia, North Cyprus, Mersin 10, Turkey
- <sup>55</sup> University of Chinese Academy of Sciences, Beijing 100049, People's Republic of China
- <sup>56</sup> University of Groningen, NL-9747 AA Groningen, The Netherlands
- <sup>57</sup> University of Hawaii, Honolulu, Hawaii 96822, USA
- <sup>58</sup> University of Jinan, Jinan 250022, People's Republic of China
- <sup>59</sup> University of Manchester, Oxford Road, Manchester, M13 9PL, United Kingdom
- <sup>60</sup> University of Minnesota, Minneapolis, Minnesota 55455, USA
- <sup>61</sup> University of Muenster, Wilhelm-Klemm-Str. 9, 48149 Muenster, Germany
- <sup>62</sup> University of Oxford, Keble Rd, Oxford, UK OX13RH
- <sup>63</sup> University of Science and Technology Liaoning, Anshan 114051, People's Republic of China
- <sup>64</sup> University of Science and Technology of China, Hefei 230026, People's Republic of China
- <sup>65</sup> University of South China, Hengyang 421001, People's Republic of China
- <sup>66</sup> University of the Punjab, Lahore-54590, Pakistan
- <sup>67</sup> University of Turin and INFN, (A)University of Turin, I-10125, Turin, Italy; (B)University of Eastern Piedmont, I-15121, Alessandria, Italy; (C)INFN, I-10125, Turin, Italy
- <sup>68</sup> Uppsala University, Box 516, SE-75120 Uppsala, Sweden
- <sup>69</sup> Wuhan University, Wuhan 430072, People's Republic of China
- <sup>70</sup> Xinyang Normal University, Xinyang 464000, People's Republic of China
- <sup>71</sup> Yunnan University, Kunming 650500, People's Republic of China
- <sup>72</sup> Zhejiang University, Hangzhou 310027, People's Republic of China
- <sup>73</sup> Zhengzhou University, Zhengzhou 450001, People's Republic of China
- <sup>a</sup> Also at the Moscow Institute of Physics and Technology, Moscow 141700, Russia
- <sup>b</sup> Also at the Novosibirsk State University, Novosibirsk, 630090, Russia
- <sup>c</sup> Also at the NRC "Kurchatov Institute", PNPI, 188300, Gatchina, Russia
- <sup>d</sup> Currently at Istanbul Arel University, 34295 Istanbul, Turkey
- <sup>e</sup> Also at Goethe University Frankfurt, 60323 Frankfurt am Main, Germany
- <sup>f</sup> Also at Key Laboratory for Particle Physics, Astrophysics and Cosmology, Ministry of Education; Shanghai Key Laboratory for Particle Physics and Cosmology; Institute of Nuclear and Particle Physics, Shanghai 200240, People's Republic of China

<sup>g</sup> Also at Key Laboratory of Nuclear Physics and Ion-beam Application (MOE) and Institute of Modern Physics, Fudan University, Shanghai 200443, People's Republic of China

<sup>h</sup> Also at Harvard University, Department of Physics, Cambridge, MA, 02138, USA

<sup>i</sup> Also at State Key Laboratory of Nuclear Physics and Technology, Peking University, Beijing 100871, People's Republic of China

<sup>j</sup> Also at School of Physics and Electronics, Hunan University, Changsha 410082, China

<sup>k</sup> Also at Guangdong Provincial Key Laboratory of Nuclear Science, Institute of Quantum Matter, South China Normal University, Guangzhou 510006, China

<sup>l</sup> Also at Frontiers Science Center for Rare Isotopes, Lanzhou University, Lanzhou 730000, People's Republic of China

<sup>m</sup> Also at Lanzhou Center for Theoretical Physics, Lanzhou University, Lanzhou 730000, People's Republic of China

<sup>n</sup> Also at the Department of Mathematical Sciences, IBA, Karachi, Pakistan

The cross section of the process  $e^+e^- \rightarrow \omega\pi^0\pi^0$  is measured at nineteen center-of-mass energies from 2.00 to 3.08 GeV using data collected with the BESIII detector at the BEPCII storage ring. A resonant structure around 2.20 GeV is observed with significance larger than  $5\sigma$ . Using a coherent fit to the cross section line shape, the mass and width are determined to be  $M = 2223 \pm 16 \pm 11$  MeV/ $c^2$  and  $\Gamma = 51 \pm 29 \pm 21$  MeV, respectively, where the first uncertainties are statistical and the second ones are systematic.

## I. INTRODUCTION

The process  $e^+e^- \rightarrow V\pi\pi$ , where  $V$  denotes a vector meson state, has been widely studied and provides an important arena for the measurements of resonant structures. For example, there are bottomonium states in the process  $e^+e^- \rightarrow \Upsilon(nS)\pi^+\pi^-$  [1], charmonium states in the  $e^+e^- \rightarrow J/\psi\pi\pi$  and  $\psi(2S)\pi\pi$  processes [2–5], and  $\phi(2170)$  in  $e^+e^- \rightarrow \phi\pi^+\pi^-$  [6, 7]. Hence, it is natural to search for vector mesons in  $e^+e^- \rightarrow \omega\pi\pi$  processes. According to isospin conservation in strong interactions and the Clebsch-Gordon coefficients involved, of the two intermediate-state isospin possibilities,  $I = 0$  and  $I = 1$ , both are allowed for the process  $e^+e^- \rightarrow \omega\pi^+\pi^-$ , while only  $I = 0$  is allowed for  $e^+e^- \rightarrow \omega\pi^0\pi^0$ , which makes the  $\omega\pi^0\pi^0$  channel most suitable to search for an intermediate isoscalar resonance.

The BABAR collaboration has used the initial state radiation method to measure the cross sections of various processes in the low energy region below 2.2 GeV [8, 9]. More recently they have expanded their measurements up to 2.5 GeV and used the results in conjunction with their previous results to investigate the nature of the resonance observed by the BESIII collaboration in the  $e^+e^- \rightarrow K^+K^-$  cross section near 2.2 GeV [10]. Among the cross sections measured by BABAR were the processes  $e^+e^- \rightarrow \omega\pi^+\pi^-$  and  $\omega\pi^0\pi^0$  [8, 9], where they reported a resonant structure with a mass of  $2265 \pm 20$  MeV/ $c^2$ , a width of  $75_{-27}^{+125}$  MeV, and a significance of  $2.6\sigma$ , by combining the  $\omega\pi^0\pi^0$  and  $\omega\pi^+\pi^-$  channels [11].

Since  $\phi \rightarrow \omega\pi^0\pi^0$  is an Okubo-Zweig-Iizuka (OZI) suppressed process, a resonant structure in  $e^+e^- \rightarrow \omega\pi^0\pi^0$  is more likely to be an  $\omega$  excited state than a  $\phi$  excited state. According to the Particle Data Group (PDG) [12], there are three  $\omega$  excited state candidates around 2.2 GeV,  $\omega(2205)$  [13],  $\omega(2290)$  [14] and  $\omega(2330)$  [15], which are not fully understood yet. Ref. [16] predicts these to be  $n^3S_1$

states for  $\omega(2290)$  and  $\omega(2330)$  and an  $n^3D_1$  state for  $\omega(2205)$ . Further experimental investigations are needed to disentangle this scenario.

In this paper, the Born cross sections of the process  $e^+e^- \rightarrow \omega\pi^0\pi^0$  are measured with data samples collected at nineteen center-of-mass energies ( $\sqrt{s}$ ) from 2.00 to 3.08 GeV corresponding to a total integrated luminosity of  $647$  pb $^{-1}$ . With the same data samples, several other hadronic processes have been used to search for excited meson states above 2.0 GeV, including  $e^+e^- \rightarrow \eta'\pi^+\pi^-$ ,  $\omega\pi^0$ ,  $\omega\eta$ , etc [10, 17–22].

## II. DETECTOR AND DATA SAMPLE

The BESIII detector [23] records symmetric  $e^+e^-$  collisions provided by the BEPCII storage ring [24], which operates in the center-of-mass energy range from 2.0 to 4.95 GeV. BESIII has collected large data samples in this energy region [25]. The cylindrical core of the BESIII detector covers 93% of the full solid angle and consists of a helium-based multilayer drift chamber (MDC), a plastic scintillator time-of-flight system (TOF), and a CsI(Tl) electromagnetic calorimeter (EMC), which are all enclosed in a superconducting solenoidal magnet providing a 1.0 T magnetic field. The solenoid is supported by an octagonal flux-return yoke with resistive plate counter muon identification modules interleaved with steel. The charged-particle momentum resolution at 1 GeV/ $c$  is 0.5%, and the  $dE/dx$  resolution is 6% for electrons from Bhabha scattering. The EMC measures photon energies with a resolution of 2.5% (5%) at 1 GeV in the barrel (end cap) region. The time resolution in the TOF barrel region is 68 ps, while that in the end cap region is 110 ps.

Simulated data samples produced with a GEANT4-based [26] Monte Carlo (MC), which includes the geometric description of the BESIII detector and the detec-

tor response, are used to determine detection efficiencies and to estimate backgrounds. The known decay modes are modeled with EVTGEN [27] using branching fractions taken from the PDG [12]. Final state radiation (FSR) from charged final state particles is incorporated using PHOTOS [28], and initial state radiation (ISR) is incorporated using ConExc [29]. The  $\omega\pi^0\pi^0$  state is simulated by using a uniformly distributed phase space (PHSP) model. The decay of  $\omega$  to  $\pi^+\pi^-\pi^0$  is analyzed using a Dalitz plot analysis [30]. Inclusive MC events for studying background contamination are generated using a hybrid generator [31], which includes hadronic events and background events.

### III. EVENT SELECTION AND BACKGROUND ANALYSIS

For the process  $e^+e^- \rightarrow \omega\pi^0\pi^0$ , with subsequent decays  $\omega \rightarrow \pi^+\pi^-\pi^0$  and  $\pi^0 \rightarrow \gamma\gamma$ , candidate events are required to have two reconstructed charged tracks and at least six reconstructed photons. Charged tracks detected in the MDC are required to be within a polar angle ( $\theta$ ) range of  $|\cos\theta| < 0.93$ , where  $\theta$  is defined with respect to the  $z$ -axis, which is the symmetry axis of the MDC. The distance of closest approach to the interaction point must be less than 10 cm along the  $z$ -axis and less than 1 cm in the transverse plane. Photon candidates are identified using showers in the EMC. The deposited energy of each shower must be more than 25 MeV in the barrel region ( $|\cos\theta| < 0.80$ ) and more than 50 MeV in the end cap region ( $0.86 < |\cos\theta| < 0.92$ ). To exclude showers that originate from charged tracks, the angle between the position of each shower in the EMC and the closest extrapolated charged track must be greater than 10 degrees. To suppress electronic noise and showers unrelated to the event, the difference between the EMC time and the event start time is required to be within  $[0, 700]$  ns.

Particle identification (PID) for charged tracks combines measurements of  $dE/dx$  in the MDC and the flight time in the TOF to form likelihoods  $\mathcal{L}(h)$  ( $h = p, K, \pi$ ) for each hadron  $h$  hypothesis. Tracks are identified as pions when the pion hypothesis has the greatest likelihood ( $\mathcal{L}(\pi) > \mathcal{L}(K)$  and  $\mathcal{L}(\pi) > \mathcal{L}(p)$ ). Two identified charged pions are required and then used in a vertex fit. Only events with two charged pions satisfying the vertex fit are selected.

To suppress background events, a four-constraint (4C) kinematic fit imposing four-momentum conservation is performed under the hypothesis  $e^+e^- \rightarrow \omega\pi^0\pi^0 \rightarrow \pi^+\pi^-\gamma\gamma\gamma\gamma$ , with  $\chi_{4C}^2 < 100$  required, where  $\chi_{4C}^2$  is the  $\chi^2$  from the kinematic fit. For events with more than 6 photon candidates, the combination with the smallest  $\chi_{4C}^2$  is retained. Three photon pairs corresponding to the three  $\pi^0$  candidates are selected by choosing the combination with the smallest value of  $\chi_{\pi^0\pi^0\pi^0}^2 = (M(\gamma_1\gamma_2) - M_{\pi^0}^{\text{PDG}})^2/\sigma_{\gamma_1\gamma_2}^2 + (M(\gamma_3\gamma_4) - M_{\pi^0}^{\text{PDG}})^2/\sigma_{\gamma_3\gamma_4}^2 +$

$(M(\gamma_5\gamma_6) - M_{\pi^0}^{\text{PDG}})^2/\sigma_{\gamma_5\gamma_6}^2$ , where  $M_{\pi^0}^{\text{PDG}}$  is the mass of  $\pi^0$  from the PDG [12] and  $\sigma_{\gamma_i\gamma_j}$  are the calculated standard deviations of  $\gamma\gamma$  invariant mass distributions from MC samples. Of the three  $\pi^0$  mesons, the one with the minimum  $|M_{\pi^+\pi^-\pi^0} - M_{\omega}^{\text{PDG}}|$  is assigned to be from the  $\omega$  decay and tagged as  $\pi_1^0$ , where  $M_{\omega}^{\text{PDG}}$  is the mass of  $\omega$  from the PDG [12]. The two photons used to reconstruct  $\pi_1^0$  are tagged as  $\gamma_1$  and  $\gamma_2$ . The other two  $\pi^0$  mesons are tagged as  $\pi_2^0$  and  $\pi_3^0$  according to  $M_{\omega\pi_2^0} < M_{\omega\pi_3^0}$ , where  $M_{\omega\pi_2^0}$  and  $M_{\omega\pi_3^0}$  represent the invariant mass of  $\omega\pi_2^0$  and  $\omega\pi_3^0$ , respectively. The photons used to reconstruct them are tagged as  $\gamma_3, \gamma_4, \gamma_5$  and  $\gamma_6$ , respectively.

The difference between the invariant mass of the reconstructed  $\pi^0$  and  $M_{\pi^0}^{\text{PDG}}$  is required to be less than 3 times the left (right) side standard deviation:  $M_{\gamma_i\gamma_j} \in [M_{\pi^0}^{\text{PDG}} - 3 \cdot \sigma_{(\text{left})\gamma_i\gamma_j}, M_{\pi^0}^{\text{PDG}} + 3 \cdot \sigma_{(\text{right})\gamma_i\gamma_j}]$ , where  $\sigma_{(\text{left})}$  and  $\sigma_{(\text{right})}$  are the quadratic means of the difference of the mass of the reconstructed  $\pi^0$  and  $M_{\pi^0}^{\text{PDG}}$  for events with mass above and below  $M_{\pi^0}^{\text{PDG}}$ , respectively.

The invariant mass distribution of the reconstructed  $\omega$  candidates at  $\sqrt{s} = 2.1250$  GeV is shown in Fig. 1. There are contributions from both  $\omega$  and backgrounds. In this distribution,  $|M_{\pi^+\pi^-\gamma_1\gamma_2} - M_{\omega}^{\text{PDG}}| < 0.05$  GeV/ $c^2$  is chosen as the signal region, while  $|M_{\pi^+\pi^-\gamma_1\gamma_2} - M_{\omega}^{\text{PDG}}| \in [0.10, 0.20]$  GeV/ $c^2$  is chosen as the sideband region to estimate backgrounds, as shown in Fig. 1.

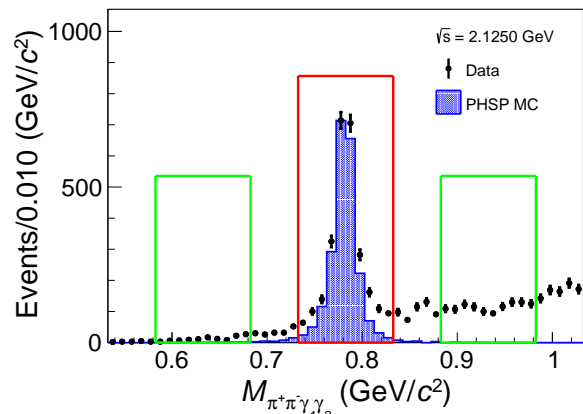


FIG. 1. The invariant mass distribution of  $\pi^+\pi^-\gamma_1\gamma_2$  at  $\sqrt{s} = 2.1250$  GeV. The black dots with error bars are data. The blue histogram represents the contribution of the signal process. The red box indicates the signal region while the green boxes indicate the sideband region.

Inclusive MC events are selected with the same event selection criteria. Detailed event type analysis over these events with TopoAna [32], shows that the dominant backgrounds come from processes with  $\pi^+\pi^-\pi^0\pi^0\pi^0$  final states but through different intermediate states. However, no peaking background appears under the  $\omega$  resonance.

#### IV. BORN CROSS SECTION MEASUREMENT

The Born cross section of  $e^+e^- \rightarrow \omega\pi^0\pi^0$  is calculated from

$$\sigma^B = \frac{N_{\text{signal}}}{\mathcal{L} \cdot \varepsilon \cdot \mathcal{B}_{\omega \rightarrow \pi^+\pi^-\pi^0} \cdot \mathcal{B}_{\pi^0 \rightarrow \gamma\gamma}^3 \cdot (1 + \delta)}, \quad (1)$$

where  $\mathcal{L}$  is the luminosity,  $N_{\text{signal}}$  is the signal yield,  $\varepsilon$  is the detection efficiency and  $\mathcal{B}_{\omega \rightarrow \pi^+\pi^-\pi^0}$  and  $\mathcal{B}_{\pi^0 \rightarrow \gamma\gamma}$  are branching fractions taken from the PDG [12]. The product of the ISR correction factor times the vacuum-polarization (VP) correction factor is represented by  $1 + \delta$ .

The PHSP MC samples are found to strongly deviate from the data. To obtain a more reliable detection efficiency, the PHSP MC events are weighted according to the two-dimension distribution of  $M_{\pi^+\pi^-\gamma_1\gamma_2\gamma_3\gamma_4}$  versus  $M_{\gamma_3\gamma_4\gamma_5\gamma_6}$ , where the weight factor is the ratio between data and the PHSP MC in this distribution. It is defined as  $w = (n_{\text{Data}} - n_{\text{Sideband}})/n_{\text{MC}}$ , where  $n$  denotes the number of events in the corresponding region. Good agreement between data and weighted MC distributions is observed, as shown in Fig. 2. The detection efficiency ( $\varepsilon$ ) is taken as the total weight of selected events divided by the total weight of generated events.

The signal yield of  $e^+e^- \rightarrow \omega\pi^0\pi^0$  is obtained by fitting the  $\pi^+\pi^-\gamma_1\gamma_2$  mass spectrum with an unbinned maximum likelihood method. The contribution of background events is described by a linear function, and the  $\omega$  signal is described by the MC-simulated shape convolved with a Gaussian function which accounts for the difference between MC and data. Figure 3 shows the fitted  $\pi^+\pi^-\gamma_1\gamma_2$  mass spectrum for the data sample at  $\sqrt{s} = 2.1250$  GeV.

The ISR and VP effects are incorporated by ConExc [29], which provides ISR and VP factors depending on the input cross section. An iterative procedure is performed, with comparison between the input cross sections and the measured ones, until the difference of  $(1 + \delta)$  is less than 1% between the last two iterations.

The Born cross sections for all nineteen energies together with all values used in the measurement are shown in Table I.

#### V. SYSTEMATIC UNCERTAINTY

Several sources of systematic uncertainties, which include the luminosity measurements, tracking efficiency, PID efficiency, photon detection, kinematic fit,  $\gamma\gamma$  mass requirement, fitting procedure, branching fractions of intermediate state decays and the ISR and VP corrections, are considered in this analysis.

(a) The integrated luminosities of the data samples used in this analysis are measured using large angle Bhabha scattering events, and the corresponding uncertainties are estimated to be 1.0% [33].

(b) The uncertainty of the tracking efficiency is investigated using samples of the  $e^+e^- \rightarrow K^+K^-\pi^+\pi^-$  process [10, 34]. The difference in tracking efficiency between data and the MC simulation is estimated to be 1.0% per pion. Hence, 2.0% is taken as the systematic uncertainty.

(c) To estimate the uncertainty in the PID efficiency, the same samples as used to investigate the tracking efficiency are studied. The average difference in the PID efficiency between data and the MC simulation is found to be 1.0% per charged pion. Therefore, 2.0% is taken as the systematic uncertainty.

(d) The uncertainty associated with the photon selection efficiency is studied with samples of  $e^+e^- \rightarrow K^+K^-\pi^+\pi^-\pi^0$  [34]. The samples cover the same angle and momentum ranges as in this analysis. The result shows that the difference in detection efficiency between data and MC simulation is 1.0% per photon. The systematic uncertainty of six photons is fully correlated and result in 6.0% uncertainty in total.

(e) The uncertainty associated with the branching fractions of intermediate states are taken from the PDG as 0.7%.

(f) The uncertainty associated with the kinematic fit comes from the inconsistency of the track helix parameters between data and the MC simulation. The helix parameters for the charged tracks of MC samples are corrected to eliminate the inconsistency, as described in Ref. [35], and the agreement of the  $\chi^2_{4C}$  distributions between data and MC simulation is significantly improved. The differences of the selection efficiencies with and without the correction are taken as the systematic uncertainties.

(g) The uncertainty associated with the background shape is estimated by the difference if a second order polynomial function is used for the background shape.

(h) The uncertainty associated with the signal function in the signal determination is estimated by the difference if an alternative fit with a Breit-Wigner function convolved with a Gaussian function is used for the signal shape.

(i) The uncertainty associated with the mass window of the  $\gamma\gamma$  invariant mass distribution is estimated by changing the number of one-side standard deviations from 3 to 2.8 and 3.2. The larger difference in the calculated cross section results is taken as the systematic uncertainty.

(j) The uncertainty associated with the mass window of  $\pi^+\pi^-\gamma_1\gamma_2$  is estimated by changing the fitting range from  $M_{\omega}^{\text{PDG}} \pm 0.15$  GeV/ $c^2$  to  $M_{\omega}^{\text{PDG}} \pm 0.14$  GeV/ $c^2$  and  $M_{\omega}^{\text{PDG}} \pm 0.16$  GeV/ $c^2$ . The larger difference in the result of the calculated cross section is taken as the systematic uncertainty.

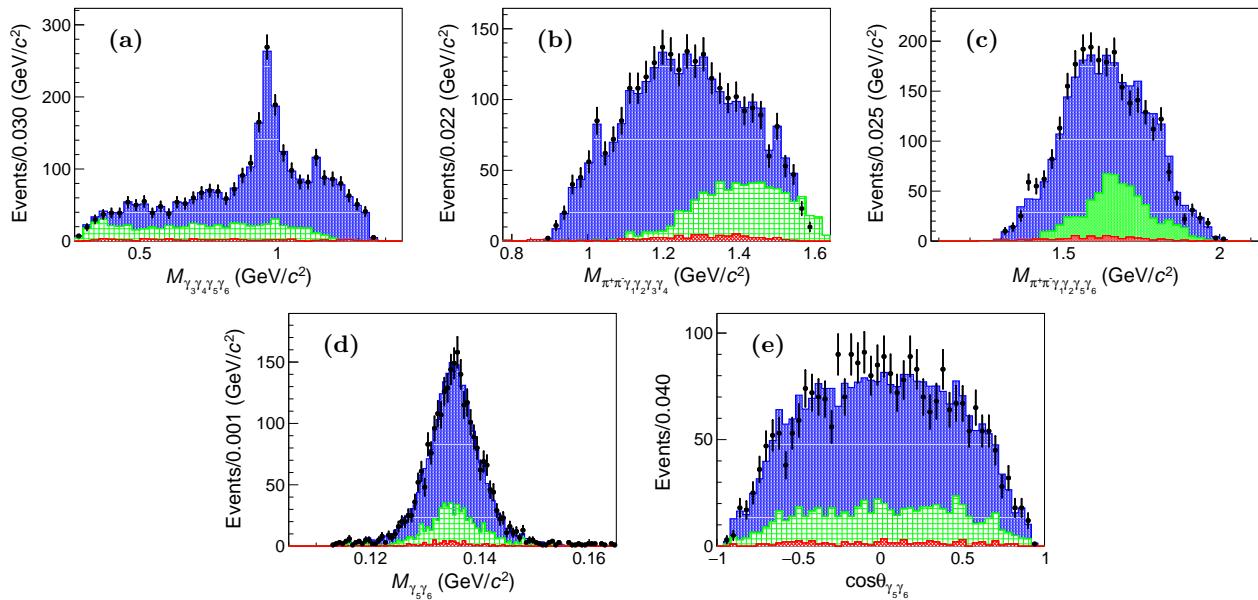


FIG. 2. The invariant mass distributions of (a)  $\gamma_3\gamma_4\gamma_5\gamma_6$ , (b)  $\pi^+\pi^-\gamma_1\gamma_2\gamma_3\gamma_4$ , (c)  $\pi^+\pi^-\gamma_1\gamma_2\gamma_5\gamma_6$ , (d)  $\gamma_5\gamma_6$ , and (e)  $\cos\theta_{\gamma_5\gamma_6}$  at  $\sqrt{s} = 2.1250$  GeV, where  $\theta_{\gamma_5\gamma_6}$  is the polar angle of the  $\gamma_5\gamma_6$  system defined with respect to the  $z$ -axis. In both (d) and (e), the distribution of  $\gamma_5\gamma_6$  is shown as an example of the three possible  $\gamma\gamma$  combinations. The black dots with error bars represent the data. The blue histogram represents the contribution of the weighted signal MC. The red and green histograms represent the contributions of estimated backgrounds, which are given by one half of the sum of the left and right sidebands in the  $\pi^+\pi^-\gamma_1\gamma_2$  invariant mass distribution, respectively. Histograms are stacked above one another to compare with data. The histograms are normalized according to the number of events in the histograms.

TABLE I. Born cross sections for  $e^+e^- \rightarrow \omega\pi^0\pi^0$ . The columns represent center-of-mass energy ( $\sqrt{s}$ ), signal yield, luminosity, detection efficiency, ISR and VP corrections and calculated Born cross section. The first uncertainties for the Born cross section are statistical, and the second ones are systematic. The uncertainties for the signal yield are statistical only.

$\sqrt{s}$ (GeV)	$N_{\text{signal}}$	$\mathcal{L}$ ( $pb^{-1}$ )	$\epsilon$	$1 + \delta$	Born cross section (pb)
2.0000	$270 \pm 18$	10.1	0.12	0.89	$293.9 \pm 20.0 \pm 20.0$
2.0500	$87 \pm 10$	3.34	0.12	0.94	$278.8 \pm 33.1 \pm 18.9$
2.1000	$252 \pm 18$	12.2	0.11	0.97	$220.6 \pm 16.0 \pm 15.3$
2.1250	$2169 \pm 54$	108.0	0.11	0.98	$213.7 \pm 5.3 \pm 14.5$
2.1500	$55 \pm 8$	2.84	0.11	0.98	$208.3 \pm 31.7 \pm 14.2$
2.1750	$237 \pm 17$	10.6	0.11	0.98	$223.8 \pm 16.2 \pm 15.2$
2.2000	$314 \pm 20$	13.7	0.12	0.97	$234.3 \pm 14.9 \pm 15.9$
2.2324	$224 \pm 16$	11.9	0.11	1.04	$185.1 \pm 13.6 \pm 12.6$
2.3094	$206 \pm 17$	21.1	0.10	1.13	$101.5 \pm 8.2 \pm 6.9$
2.3864	$194 \pm 16$	22.5	0.10	1.14	$88.3 \pm 7.3 \pm 6.0$
2.3960	$530 \pm 27$	66.9	0.10	1.14	$77.3 \pm 3.9 \pm 5.3$
2.6444	$206 \pm 16$	33.7	0.10	1.25	$59.1 \pm 4.6 \pm 4.0$
2.6464	$192 \pm 15$	34.0	0.10	1.28	$55.8 \pm 4.5 \pm 3.8$
2.9000	$299 \pm 19$	105.0	0.10	1.34	$25.6 \pm 1.6 \pm 1.7$
2.9500	$33 \pm 7$	15.9	0.10	1.33	$20.5 \pm 4.2 \pm 1.4$
2.9810	$52 \pm 8$	16.1	0.10	1.38	$30.4 \pm 4.8 \pm 2.1$
3.0000	$28 \pm 6$	15.9	0.10	1.29	$15.9 \pm 3.6 \pm 1.1$
3.0200	$31 \pm 6$	17.3	0.09	1.34	$15.9 \pm 3.1 \pm 1.1$
3.0800	$158 \pm 15$	126.0	0.09	1.34	$12.9 \pm 1.2 \pm 0.9$

(k) The uncertainty associated with  $1 + \delta$  is obtained from the accuracy of the radiation function, which is about 0.5% [36], and the contribution from the cross sec-

tion lineshape, which is estimated by varying the model parameters of the fit to the cross section. All parameters are randomly varied within their uncertainties, and

TABLE II. Systematic uncertainties (in percentage) in this analysis. The columns represent center-of-mass energy ( $\sqrt{s}$ ), the uncertainty associated with luminosity, charged track selection, PID, photon selection, branching fraction, 4C kinematic fit, background shape, signal shape,  $M_{\gamma\gamma}$ ,  $M_{\pi^+\pi^-\gamma_1\gamma_2}$  invariant mass window and  $1 + \delta$  calculation. The last column is the total systematic uncertainty.

$\sqrt{s}$ (GeV)	$\mathcal{L}$	Charged track selection		Photon selection	Branching fraction	4C kinematic fit	Background shape	Signal shape	$M_{\gamma\gamma}$ window	$M_{\pi^+\pi^-\gamma_1\gamma_2}$ window	$1 + \delta$	Total
2.0000	1.0	2.0	2.0	6.0	0.7	0.57	0.22	0.13	0.18	0.18	0.5	6.80
2.0500	1.0	2.0	2.0	6.0	0.7	0.55	0.10	0.18	0.16	0.18	0.5	6.79
2.1000	1.0	2.0	2.0	6.0	0.7	0.66	0.17	1.43	0.11	0.11	0.5	6.95
2.1250	1.0	2.0	2.0	6.0	0.7	0.36	0.19	0.41	0.26	0.17	0.5	6.79
2.1500	1.0	2.0	2.0	6.0	0.7	0.68	0.12	0.45	0.14	0.14	0.5	6.82
2.1750	1.0	2.0	2.0	6.0	0.7	0.46	0.11	0.18	0.11	0.18	0.5	6.79
2.2000	1.0	2.0	2.0	6.0	0.7	0.52	0.19	0.14	0.15	0.16	0.5	6.79
2.2324	1.0	2.0	2.0	6.0	0.7	0.47	0.14	0.15	0.17	0.52	0.5	6.80
2.3094	1.0	2.0	2.0	6.0	0.7	0.36	0.93	0.16	0.18	0.16	0.5	6.84
2.3864	1.0	2.0	2.0	6.0	0.7	0.34	0.14	0.17	0.11	0.13	0.5	6.78
2.3960	1.0	2.0	2.0	6.0	0.7	0.54	0.11	0.24	0.47	0.10	0.5	6.81
2.6444	1.0	2.0	2.0	6.0	0.7	0.39	0.17	0.26	0.32	0.36	0.5	6.80
2.6464	1.0	2.0	2.0	6.0	0.7	0.60	0.13	0.29	0.10	0.16	0.5	6.80
2.9000	1.0	2.0	2.0	6.0	0.7	0.23	0.17	0.14	0.17	0.15	0.5	6.77
2.9500	1.0	2.0	2.0	6.0	0.7	0.49	0.18	1.48	0.61	0.77	0.5	7.01
2.9810	1.0	2.0	2.0	6.0	0.7	0.50	0.14	0.13	0.13	0.11	0.5	6.79
3.0000	1.0	2.0	2.0	6.0	0.7	0.64	0.13	1.06	0.13	0.66	0.5	6.91
3.0200	1.0	2.0	2.0	6.0	0.7	0.26	0.14	0.11	0.12	0.17	0.5	6.77
3.0800	1.0	2.0	2.0	6.0	0.7	0.35	0.11	0.13	0.15	0.10	0.5	6.78

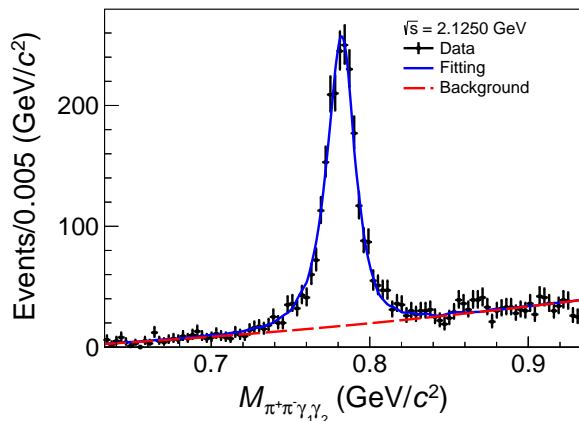


FIG. 3. Fitting result for the  $\pi^+\pi^-\gamma_1\gamma_2$  mass spectrum for the data sample at  $\sqrt{s} = 2.1250$  GeV. Dots with error bars represent data. The blue solid line represents the fitting function, and the red dashed line represents the background.

the resulted parametrization of the lineshape is used to recalculate  $1 + \delta$ ,  $\epsilon$  and the corresponding cross section. This procedure is repeated 100 times, and the standard deviation of the resulting cross section is taken as the systematic uncertainty.

All systematic uncertainties are summarized in Table II. The total systematic uncertainty is obtained by adding all individual contributions in quadrature.

## VI. LINESHAPE FITTING TO THE CROSS SECTION

To study the possible structure around 2.20 GeV, the cross section  $\sigma^B(s)$  is fitted by the coherent sum of the possible resonant component together with a phase space component for the continuum contribution:

$$\begin{aligned}
 \sigma^B(s) &= |\sigma_r(\sqrt{s})e^{i\phi_r} + \sigma_c(\sqrt{s})|^2, \\
 \sigma_r(s) &= \frac{M_r \sqrt{12\pi C \Gamma_{ee}^r Br \Gamma_r}}{\sqrt{s} s - M_r^2 + iM_r \Gamma_r} \sqrt{\frac{\Phi(\sqrt{s})}{\Phi(M_r)}}, \\
 \sigma_c(s) &= a \frac{\sqrt{\Phi(\sqrt{s})}}{(\sqrt{s})^b},
 \end{aligned} \tag{2}$$

where  $\sigma_r(s)$  represents the resonant component [37], in which  $M_r$  and  $\Gamma_r$  are the mass and width of the resonant structure near 2.20 GeV. Parameter  $\Gamma_{ee}^r Br$  is the electric partial width times the branching fraction of the resonance decaying to  $\omega\pi^0\pi^0$ ,  $\phi_r$  is the relative phase between the resonant and nonresonant amplitude, and the continuum part  $\sigma_c(s)$  is parameterized by  $a$  and  $b$ . All six parameters above are floated, while  $\Phi$  is the calculated three-body phase space factor and  $C$  is a conversion constant which equals to  $3.893 \times 10^8$  pb  $\cdot$  GeV<sup>2</sup> [8]. The results from the fit are shown in Fig. 4 and Table III. Two solutions are found. Solution (a) corresponds to the case of constructive interference between the resonant and continuum contributions and solution (b) corresponds to the case of destructive interference. The fitting

quality  $\chi^2/\text{ndf}$  is 21.2/13, where ndf is the number of degrees of freedom.

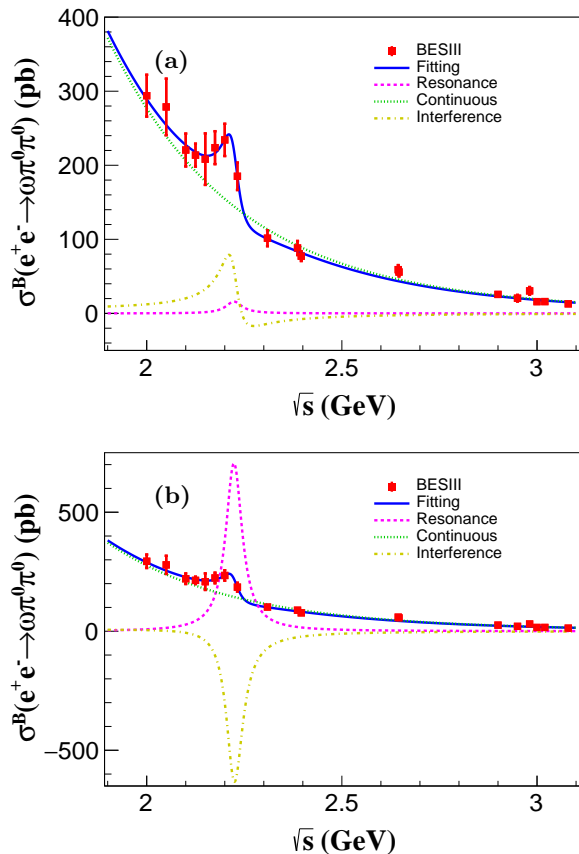


FIG. 4. Fit to the Born cross section of  $e^+e^- \rightarrow \omega\pi^0\pi^0$ . (a) The solution with constructive interference. (b) The solution with destructive interference. Red dots with error bars represent data, while blue solid line represents total fitting function, and green dotted, magenta dashed and yellow dashed curves represent the contributions of nonresonant, resonant and interference components, respectively.

To study the systematic uncertainties for the resonant parameters, an alternative fit is carried out by parameterizing the continuum component with an exponential function [2]:

$$\sigma_c(s) = \sqrt{\Phi(\sqrt{s})e^{p_0u}p_1}, \quad (3)$$

where  $p_0$ ,  $p_1$  are floated parameters and  $u = \sqrt{s} - (2M_{\pi_0}^{\text{PDG}} + M_{\omega}^{\text{PDG}})$ . The differences of the results between the alternative fit with Eq. (3) for the continuum component and the nominal fit are taken as systematic uncertainties for the resonant parameters. The systematic uncertainties associated with the signal model are also studied by using a relativistic Breit-Wigner function with an energy-dependent width as the signal shape [12]. They are found to be negligible. Finally, the

TABLE III. The result of the fit to the  $e^+e^- \rightarrow \omega\pi^0\pi^0$  cross section with functions described by Eq. (2). The uncertainty is statistical only. The statistical significance is calculated from the difference in  $\chi^2$  of the fit if only the continuum shape is used to fit the Born cross sections.

Parameter	Solution (a)	Solution (b)
$M_r$ (MeV/ $c^2$ )	$2223 \pm 16$	
$\Gamma_r$ (MeV)	$51 \pm 29$	
$\phi_r$	$2.5 \pm 0.3$	$-1.7 \pm 0.1$
$\Gamma_{ee}^r Br$ (eV)	$0.3 \pm 0.1$	$12.2 \pm 6.5$
$a(\times 10^3)$		$1.3 \pm 0.1$
$b$		$5.0 \pm 0.1$
Significance		$5.4\sigma$

mass and width of the resonance are determined to be  $M = 2223 \pm 16 \pm 11$  MeV/ $c^2$  and  $\Gamma = 51 \pm 29 \pm 21$  MeV with a statistical significance of  $5.4\sigma$ , where the significance is calculated from the change in  $\chi^2$  of the fit if the resonant contribution is removed. In addition,  $\Gamma_{e^+e^-}^r Br$  is determined to be  $0.3 \pm 0.1 \pm 0.1$  eV or  $12.2 \pm 6.5 \pm 4.9$  eV for the two solutions from the fit, where the first uncertainties are statistical and the second ones are systematic.

## VII. CONCLUSION

The cross section of the process  $e^+e^- \rightarrow \omega\pi^+\pi^-$  is measured at nineteen center-of-mass energies from 2.00 to 3.08 GeV with a total integrated luminosity of  $647 \text{ pb}^{-1}$ . The resonant structure around 2.20 GeV is observed with a statistical significance of  $5.4\sigma$  in the coherent fit to the cross section line shape. The resonance has a mass of  $M = 2223 \pm 16 \pm 11$  MeV/ $c^2$  and a width of  $\Gamma = 51 \pm 29 \pm 21$  MeV, where the first uncertainties are statistical and the second ones are systematic. The resonance observed in this analysis, which could be an  $\omega$  excited state, is consistent with *BABAR*'s measurement [11]. A future study of this channel with more data sets around  $\sqrt{s} = 2.2$  GeV will be helpful to improve knowledge of this resonance [25].

## VIII. ACKNOWLEDGEMENTS

The BESIII collaboration thanks the staff of BEPCII and the IHEP computing center and the supercomputing center of USTC for their strong support. This work is supported in part by National Key R&D Program of China under Contracts Nos. 2020YFA0406400, 2020YFA0406300; National Natural Science Foundation of China (NSFC) under Contracts Nos. 11335008, 11625523, 11635010, 11735014, 11822506, 11835012, 11935015, 11935016, 11935018, 11961141012, 12022510,

12025502, 12035009, 12035013, 12061131003, 11705192, 11950410506, 12061131003; the Chinese Academy of Sciences (CAS) Large-Scale Scientific Facility Program; Joint Large-Scale Scientific Facility Funds of the NSFC and CAS under Contracts Nos. U1732263, U1832207, U1832103, U2032111; CAS Key Research Program of Frontier Sciences under Contract No. QYZDJ-SSW-SLH040; 100 Talents Program of CAS; INPAC and Shanghai Key Laboratory for Particle Physics and Cosmology; ERC under Contract No. 758462; European Union Horizon 2020 research and innovation programme under Contract No. Marie Skłodowska-Curie grant agreement No 894790; German Research Foundation DFG un-

der Contracts Nos. 443159800, Collaborative Research Center CRC 1044, FOR 2359, FOR 2359, GRK 214; Istituto Nazionale di Fisica Nucleare, Italy; Ministry of Development of Turkey under Contract No. DPT2006K-120470; National Science and Technology fund; Olle Engkvist Foundation under Contract No. 200-0605; STFC (United Kingdom); The Knut and Alice Wallenberg Foundation (Sweden) under Contract No. 2016.0157; The Royal Society, UK under Contracts Nos. DH140054, DH160214; The Swedish Research Council; U. S. Department of Energy under Contracts Nos. DE-FG02-05ER41374, DE-SC-0012069.

- 
- [1] K. F. Chen *et al.* (Belle Collaboration), *Phys. Rev. Lett.* **100**, 112001 (2008).
- [2] M. Ablikim *et al.* (BESIII Collaboration), *Phys. Rev. Lett.* **118**, 092001 (2017).
- [3] M. Ablikim *et al.* (BESIII Collaboration), *Phys. Rev. D* **102**, 012009 (2020).
- [4] M. Ablikim *et al.* (BESIII Collaboration), *Phys. Rev. D* **96**, 032004 (2017).
- [5] M. Ablikim *et al.* (BESIII Collaboration), *Phys. Rev. D* **97**, 052001 (2018).
- [6] C. P. Shen *et al.* (Belle Collaboration), *Phys. Rev. D* **80**, 031101 (2009).
- [7] M. Ablikim *et al.* (BESIII Collaboration), (2021), [arXiv:2112.13219 \[hep-ex\]](https://arxiv.org/abs/2112.13219).
- [8] B. Aubert *et al.* (BABAR Collaboration), *Phys. Rev. D* **76**, 092005 (2007).
- [9] J. P. Lees *et al.* (BABAR Collaboration), *Phys. Rev. D* **98**, 112015 (2018).
- [10] M. Ablikim *et al.* (BESIII Collaboration), *Phys. Rev. D* **99**, 032001 (2019).
- [11] J. P. Lees *et al.* (BABAR Collaboration), *Phys. Rev. D* **101**, 012011 (2020).
- [12] P. A. Zyla *et al.* (Particle Data Group), *Prog. Theor. Exp. Phys.* **2020**, 083C01 (2020).
- [13] A. V. Anisovich *et al.*, *Phys. Lett. B* **542**, 19 (2002).
- [14] D. V. Bugg, *Eur. Phys. J. C* **36**, 161 (2004).
- [15] M. Atkinson *et al.* (Omega Photon Collaboration), *Z. Phys. C* **38**, 535 (1988).
- [16] C. Q. Pang *et al.*, *Phys. Rev. D* **101**, 074022 (2020).
- [17] M. Ablikim *et al.* (BESIII Collaboration), *Phys. Rev. D* **103**, 072007 (2021).
- [18] M. Ablikim *et al.* (BESIII Collaboration), *Phys. Rev. Lett.* **124**, 112001 (2020).
- [19] M. Ablikim *et al.* (BESIII Collaboration), *Phys. Lett. B* **813**, 136059 (2021).
- [20] M. Ablikim *et al.* (BESIII Collaboration), *Phys. Rev. D* **104**, 032007 (2021).
- [21] M. Ablikim *et al.* (BESIII Collaboration), *Phys. Rev. D* **102**, 012008 (2020).
- [22] M. Ablikim *et al.* (BESIII Collaboration), *Phys. Rev. D* **100**, 032009 (2019).
- [23] M. Ablikim *et al.* (BESIII Collaboration), *Nucl. Instrum. Meth. A* **614**, 345 (2010).
- [24] C. H. Yu *et al.*, *Proceedings of IPAC2016, Busan, Korea (2016)*, 10.18429/JACoW-IPAC2016-TUYA01.
- [25] M. Ablikim *et al.* (BESIII Collaboration), *Chin. Phys. C* **44**, 040001 (2020).
- [26] S. Agostinelli *et al.* (GEANT4 Collaboration), *Nucl. Instrum. Meth. A* **506**, 250 (2003).
- [27] R. G. Ping, *Chin. Phys. C* **32**, 599 (2008).
- [28] E. Richter-Was, *Phys. Lett. B* **303**, 163 (1993).
- [29] R. G. Ping, *Chin. Phys. C* **38**, 083001 (2014).
- [30] M. Ablikim *et al.* (BESIII Collaboration), *Phys. Rev. D* **98**, 112007 (2018).
- [31] R. G. Ping *et al.*, *Chin. Phys. C* **40**, 113002 (2016).
- [32] X. Zhou, S. Du, G. Li, and C. Shen, *Comput. Phys. Commun.* **258**, 107540 (2021).
- [33] M. Ablikim *et al.* (BESIII Collaboration), *Chin. Phys. C* **41**, 063001 (2017).
- [34] W. L. Yuan *et al.*, *Chin. Phys. C* **40**, 026201 (2016).
- [35] M. Ablikim *et al.* (BESIII Collaboration), *Phys. Rev. D* **87**, 012002 (2013).
- [36] R. G. Ping, *Chin. Phys. C* **38**, 083001 (2014).
- [37] C. P. Shen and C. Z. Yuan, *Chin. Phys. C* **34**, 1045 (2010).